Appl. Math. J. Chinese Univ.
2026, 41(1): 161-180

Heat transfer analysis of Al_2O_3 and Cu nanoparticles using ethylene glycol as base fluid: A comparative study

R. Arpitha D. Srikanth*

Abstract. Currently, researchers worldwide are conducting theoretical and experimental studies to understand the significance of nanofluids in heat transfer processes. These fluids are created by dispersing nanoparticles in a base fluid. Experiments have demonstrated that nanofluids exhibit superior and more attractive thermal properties compared to conventional fluids. In this current study, we discuss about the heat transfer enhancement of unsteady incompressible laminar couple stress nanofluid flow with Magnetohydrodynamics (MHD) between parallel plates. Prescribed temperature boundary conditions of the surface are employed on the porous surface and it is assumed that the temperature changes periodically over time on the plates. The flow is provoked by periodic suction as well as injection at the plates. With the aid of similarity variables, the system of governing transport equations is transformed into a nonlinear system of ordinary differential equations which is subsequently solved using shooting method along with Runge-Kutta fourth order scheme. The obtained results are shown graphically and explained for the non-dimensional velocity, heat profiles with diverse fluid parameters as well as geometric parameters. Nusselt number is calculated at the lower and upper plates. It is found that temperature component of the fluid is augmenting with suction-injection parameter, whereas it is decreasing in nature with respect to Reynolds number.

Nomenclature

T^* dimensionless temperature, $\frac{T-T_1e^{i\omega t}}{(T-T_2)e^{i\omega t}}$
Da Darcy parameter
Ec Eckert number, $\frac{\mu v_2}{\rho hc(T_2-T_1)}$
p fluid pressure
T Temperature
h distance between parallel plates
Re Reynolds number, $\frac{\rho v_2 h}{\mu}$
k_1 permeability parameter

Received: 2022-12-27. Revised: 2024-07-15.
MR Subject Classification: 35Q35, 35Q30, 76A05, 76Z05.
Keywords: couple stress nanofluid, MHD, shooting method, porous medium.
Digital Object Identifier(DOI): https://doi.org/10.1007/s11766-026-4928-7.
*Corresponding author.

$v_1 e^{i\omega t}$ Injection velocity at the lower plate
Pr Prandtl number, $\frac{\mu c}{k}$
t time
$v_2 e^{i\omega t}$ suction velocity at the upper plate
$\hat{i}$ $\hat{j}$ unit vectors along X, Y axes, respectively
v Y-direction velocity component
a suction-injection ratio
u X-direction velocity component
Greek Letters
λ non dimensional y coordinate, $\frac{y}{h}$
ξ Dimensionless axial variable, $\left(\frac{U_0}{av_2} - \frac{x}{h}\right)$
ρ_{nf} density of the nanofluid
ψ non-dimensional frequency parameter, ωt
α couple stress parameter, $\sqrt{\frac{\eta}{\mu h^2}}$
ρ_n density of the nanoparticle
μ_{nf} dynamic viscosity of the nanofluid
ρ_f density of the base fluid
Subscripts
f fluid
n_f nanofluid
f solid

§1 Introduction

In recent decades, much of the research has been focused on the flow of non-Newtonian fluids and has gained lot of attention of research workers on account of their vast applications in the area of industry, engineering physiology, as well as in biology and also due to the interesting mathematical challenges like in slurry transport, polymeric liquids, petroleum industry, shampoos, paints, soaps, tomato paste, glass fiber, paper manufacturing, etc. Some of the non-Newtonian models are shear-thinning, thixotropic, viscoelastic, short-memory and also microstructural fluid models. There may not be a single constitutive relation available for that portraying the rheological processes of actual fluids due to the complexity of fluids and hence various researchers proposed to analyze the behavior of non-Newtonian fluids stress tensor and the rate of deformation tensor relationship. One of the crucial non-Newtonian fluid model is couple stress fluid model, which was first developed by Stokes [1]. It shows the generalization of the classical viscous fluid theory by considering the polar effects with a body couples with in the fluid medium. The most crucial characteristic of those fluids is that the stress tensor is erstwhile symmetric and the behavior of flow cannot be appropriately estimated with the aid of using the classical Newtonian concept. The couple stress fluid concept contains rigid particles along with the randomly oriented particles and also it has lot of properties to provide an explanation for the conduct of rheological complicated fluids, liquid crystals, synthetic fluids, lubricants containing a bit amount of polymer suspensions, synovial fluids, electro-rheological

fluids, colloidal fluids and animal blood. An outstanding introduction of this concept is procurable in the monograph of Theories of Fluids with Microstructure an Introduction reported by Stokes [2]. Devakar and Iyengar [3] have analyzed an incompressible run-up couple stress fluid flow confined between infinite rigid parallel plates. Sarojini et al. [4] have discovered the steady magnetohydrodynamics(MHD) couple stress fluid flow among parallel porous plates channel. A significant work was done by Srinivasacharya et al. [5], where they have examined the steady state flow of couple stress fluid flow between porous parallel plates maintaining a consistent injection at the lower plate and a consistent suction at the upper plate. They obtained the solution numerically by using quasi linearization technique. Murthy and Srinivas [6] have examined as to how a transverse magnetic field would act on the flow of two immiscible couple stress fluid inside a horizontal channel. The researches associated with couple stress fluid using different geometries have been listed in the references [7, 8].

A nanofluid was first pioneered by Choi and Eastman [9]. Nanofluid is nothing but nanoparticles added to the base fluid. The nanoparticles are the particles with dimension of 10 to 1000 nm in size approximately and those are utilized in the make of nanofluids, which might be made with the aid of metals, oxides and carbon nano tubes (carbides). Some of oxide nanoparticles are ZnO, Al_2O_3 and also CuO, while some metal nanoparticles are Gold (Au), Silver (Ag). Some of the base fluids includes Ethylene glycol, water and oil. These nano-fluids when compared with the base fluid, exhibit an excessive thermal conductivity and convective heat transfer coefficient. The effect of thermal radiation on the nanofluid can be most prominent in applications of space technology and also at high operating temperature. Nanofluids have numerous engineering applications in processing of material, synthesis of material, micro fluidics and microelectronics, solid-state lighting, transportation, manufacturing, biomedical, high power X-rays, scientific measurement and medicine. Sheikholeslami and Ganji [10] have considered the heat transfer changes in nanofluid flow which is squeezed and confined between parallel plates and acquired the solution, analytically via the usage of homotopy perturbation method(HPM). Non-linear thermal radiation of MHD three-dimensional flow of nanofluid was examined by Hayat et al. [11]. The work done by different workers for heat transfer characteristic of the fluid flow along with various geometries as well as various nanofluid models are there in [12 - 30].

The term MHD(magnetofluid dynamics or hydromagnetics) was initially introduced by Alfven. In Magnetohydrodynamic magneto means magnetic field, hydro means liquid, and dynamic means movement. If we apply magnetic field on electrically conducting fluids, then it creates forces at the fluid and have an effect on the magnetic area itself is called as MHD. MHD outcomes maybe defined with the aid of using Maxwell's equations of electromagnetism and Navier-Stokes equations. The study of magnetohydrodynamic flows has won lot of interest in the previous few many years because of its tremendous applications in bioengineering as well as medical sciences and industry. Some of the magnetohydrodynamic applications are Ship propulsion, reduction of turbulent drag, granulation of metals , MHD generators, Magnetic filtration and separation, Crystal growth, Jet printers, MHD flow meters, MHD pumps, Metallurgy (casting in Fe and Al induction furnaces), Astrophysics (planetary magnetic field), Jet printers, reduction of bleeding at some stage in the surgical procedures and development of magnetic tracers, filtration and separation using magnets, Fusion reactors (blanket, limiter,

divertor) and magnetic gadgets for mobileular separation, targeted transport of drugs with the use of magnetic debris as drug carriers. A significant work was done by Attia and Kotb [31], where they have discovered heat transfer of the MHD for steady incompressible Newtonian fluid confined between two parallel plates that are infinite, insulated and horizontal, with the assumption that the upper pate is maintained at consistent velocity while the lower plate is not moving and also the viscosity of the fluid is directly proposal to temperature. Hayat et al. [32] have described the heat transfer changes on an electrically conducting peristaltic movement in incompressible viscous fluid considered in an asymmetrical channel and then by applying less Reynolds number and lengthy wavelength assumptions, the dimensionless stream function and temperature are obtained numerically. Srinivasacharya and Kaladhar [33] have examined the flow of MHD, fully developed, non-newtonian couple stress fluid by taking into account the impacts of the Hall and Ion-slip between vertical plates in parallel with consideration of heat source which is depending on temperature. The influence of flow of radiative heat transfer on hydromagnetic couple stress fluid confined between parallel plates which are porous with the assumption of non-uniform wall temperature and by employing the Eyring Powell model was studied thoroughly by Adesanya and Makinde [34]. We can observe magnetohydrodynamics studies of fluid flow in different geometries in [13, 35]. Khan et al. [36] have examined heat transfer characteristics of the non-newtonian unsteady couple stress fluid flow under the magnetic field on a rotating disk that is infinite along z-axis and obtained the solution numerically via Runge-Kutta coupled with shooting technique. Raza et al. [37] have considered the heat transfer on Copper (Cu) water nanofluid in a porous channel with stretching walls while being affected by the magnetic effect. Ojjela et al. [38] have studied the entropy generation of two dimensional flow of incompressible, unsteady, squeezing Casson fluid among parallel disks under the impact of magnetic field.

A porous medium is nothing but a material containing very small apertures which might be commonly full of fluid which is either a liquid or a gas. It is characterized by the fraction of the volume of void spaces over the total volume of the material. The properties via way of means of the porous medium are permeability, electrical conductivity and also tensile strength. On account of these traits the porous medium has vast applications in engineering, geosciences, geomechanics and bio-fluid dynamics as well as in industry. Mostly enormous range of applications of the flow through a porous material includes restoration of crude oils from the pores of reservoirs and hydrology of water, filtration of fluids, water and oils underground movement, chemical reactors and also includes seepage of water in the river beds. Raptis et al. [39] have analyzed in detail the hydromagnetic steady natural convective fulid flow through a porous medium which is bounded by two plates that are parallel. The heat transfers of MHD radiative unsteady Eyring Powell fluid flow in a porous medium under the slip conditions have been discovered by Gbadeyan and Dada [40]. Ramesh and Devakar [41] have observed peristaltic flow of couple stress fluid through a porous media in an asymmetric channel while is being influenced by magnetic field effects. Terrill and Shrestha[42] have investigated viscous incompressible two-dimensional fluid flow through a uniformly porous parallel channel, having fluid sucked or injected with different velocities.

With an inspiration from the above literature survey, the purpose of this study is to describe

the heat transfer analysis of couple stress nanofluid flow through a porous medium considered among parallel plates under the impact of electromagnetic effect. The fluid flow is generated because of periodic suction and injection. The dimensionless velocity and temperature components with respect to exceptional fluid and geometric parameters are displayed using neat graphs. This study identifies an improvement in the thermal flow rate of nanofluid between two paraelle pates.

§2 Mathematical description

We consider the unsteady incompressible couple stress nanofluid flow along a porous medium confined amid two horizontal parallel plates with the distance between the plates being h. Lower plate is at y=0 and the upper plate is at y=h as shown in Fig. 1. Let there be a periodic injection at the lower plate with velocity $v_1 e^{i\omega t}$ and periodic suction at the upper plate with velocity $v_2 e^{i\omega t}$, where $|v_2| \geq |v_1|$. Temperatures are considered as periodic type at the boundaries. The X-axis is along the direction of the primary flow and the Y-axis is perpendicular to the primary flow, as shown in Fig. 1.

The governing expressions of the couple stress nanofluid flow, under the influence of electromagnetic field are [5, 7, 8 and 10]

$$\frac{\partial u}{\partial x} + \frac{\partial v}{\partial x} = 0, \tag{1}$$

$$\begin{aligned}\rho_{nf}\left(\frac{\partial u}{\partial t} + u\frac{\partial u}{\partial x} + v\frac{\partial u}{\partial x}\right) = &-\frac{\partial p}{\partial x} + \mu_{nf}\left(\frac{\partial^2 u}{\partial x^2} + \frac{\partial^2 u}{\partial y^2}\right) - \eta\left(\frac{\partial^4 u}{\partial x^4} + \frac{\partial^4 u}{\partial y^4} + 2\frac{\partial^4 u}{\partial x^2 \partial y^2}\right)\\ &- \frac{\mu_{nf}}{K_1}u - \sigma_{nf}B_0^2 u,\end{aligned} \tag{2}$$

$$\begin{aligned}\rho_{nf}\left(\frac{\partial v}{\partial t} + u\frac{\partial v}{\partial x} + v\frac{\partial v}{\partial y}\right) = &-\frac{\partial p}{\partial y} + \mu_{nf}\left(\frac{\partial^2 v}{\partial x^2} + \frac{\partial^2 v}{\partial y^2}\right) - \eta\left(\frac{\partial^4 v}{\partial x^4} + \frac{\partial^4 v}{\partial y^4} + 2\frac{\partial^4 v}{\partial x^2 \partial y^2}\right)\\ &- \frac{\mu_{nf}}{K_1}v - \sigma_{nf}B_0^2 v,\end{aligned} \tag{3}$$

$$\begin{aligned}&(\rho c)_{nf}\left(\tfrac{\partial T}{\partial t} + v\tfrac{\partial T}{\partial y} + u\tfrac{\partial T}{\partial x}\right) = k_{nf}\left(\tfrac{\partial^2 T}{\partial x^2} + \tfrac{\partial^2 T}{\partial y^2}\right) - \mu_{nf}\left(\left(\tfrac{\partial u}{\partial x}\right)^2 + \left(\tfrac{\partial v}{\partial x}\right)^2 + \left(\tfrac{\partial u}{\partial y} + \tfrac{\partial u}{\partial x}\right)^2\right)\\ &+\eta\left(\left(\tfrac{\partial^2 u}{\partial x^2} + \tfrac{\partial^2 u}{\partial y^2}\right)^2 + \left(\tfrac{\partial^2 v}{\partial x^2} + \tfrac{\partial^2 v}{\partial y^2}\right)^2\right) + \tfrac{\mu_{nf}}{k_{nf}}\left(u^2 + v^2\right) + \sigma_{nf}B_0^2\left(u^2 + v^2\right).\end{aligned} \tag{4}$$

The velocity and temperature similarity transformations are as given below

$$u(x,\lambda,t) = f'(\lambda)\, e^{i\omega t}\left(-\frac{V_2 x}{h} + \frac{U_0}{a}\right), \tag{5}$$

$$v(x,\lambda,t) = V_2 f(\lambda)\, e^{i\omega t}$$

$$T(x,\lambda,t) = \left[T_1 + \frac{\mu v_2}{\rho h c}\left(\phi_1(\lambda) + \left(\frac{U_0}{a v_2} - \frac{x}{h}\right)^2\right)\phi_2(\lambda)\right] e^{i\omega t},$$

where $\lambda = \frac{y}{h}$. The initial and boundary conditions assumed are as follows

$$\begin{aligned}&u = 0, v = v_1 e^{i\omega t}, \nabla \times \bar{q} = 0, T = T_1 e^{i\omega t} \;\; at \;\; y = 0,\\ &u = 0, v = v_2 e^{i\omega t}, \nabla \times \bar{q} = 0, T = T_2 e^{i\omega t} \;\; at \;\; y = h.\end{aligned} \tag{6}$$

Substituting (5) in (2), (3), and (4) then we have

$$f^{v\prime}=\frac{1}{\alpha^2}\left[\frac{1}{(1-\phi)^{2.5}}f'^{v}+A_1\mathrm{Re}\left(f'f''-ff^{'''}\right)cos\omega t-\frac{1}{(1-\phi)^{2.5}}Daf''-A_4M^2f''\right], \quad (7)$$

$$\phi_1''=\frac{1}{A_3}\left[\begin{array}{l}A_2\,\mathrm{Pr}\,\mathrm{Re}\,(f\phi_1')\,cos\omega t-2A_3\phi_2-\frac{4}{(1-\phi)^{2.5}}\,\mathrm{Pr}\,\mathrm{Re}f'^2cos\omega t-\mathrm{Pr}\,Re\alpha^2f''^2cos\omega t\\ -\frac{1}{(1-\phi)^{2.5}}\frac{1}{A_3}Da\,\mathrm{Pr}\,\mathrm{Re}f^2cos\omega t-A_4M^2f^2\,\mathrm{Pr}\,Recos\omega t\end{array}\right], \quad (8)$$

$$\phi_2''=\frac{1}{A_3}\left[\begin{array}{l}A_2\,\mathrm{Pr}\,\mathrm{Re}\,(-2f'\phi_2+f\phi_2)\,cos\omega t-\frac{1}{(1-\phi)^{2.5}}\,\mathrm{Pr}\,\mathrm{Re}f^{''2}cos\omega t-\mathrm{Pr}\,Re\alpha^2f''^2cos\omega t\\ -\frac{1}{(1-\phi)^{2.5}}\frac{1}{A_3}\,\mathrm{Pr}\,\mathrm{Re}f'^2cos\omega t-A_4M^2\,\mathrm{Pr}\,\mathrm{Re}f'^2cos\omega t\end{array}\right], \quad (9)$$

$$where A_1=\frac{\rho_{nf}}{\rho_f}=(1-\phi_p)+\phi_p\frac{\rho_p}{\rho_f},A_2=\frac{(\rho c)_{nf}}{(\rho c)_f}=(1-\phi_p)+\phi_p\frac{(\rho c)_p}{(\rho c)_f},$$

$$A_3=\frac{K_{nf}}{K_f}=\frac{K_p+2K_f-2\phi_p\,(K_f-K_p)}{K_p+2K_f+\phi_p\,(K_f-K_p)},A_4=\frac{(\sigma)_{nf}}{(\sigma)_f}=1+\phi_p\frac{3\left(\frac{\sigma_{nf}}{\sigma_f}-K_p\right)}{K_p+2K_f+\phi_p\,(K_f-K_p)},$$

$$\frac{(\mu)_{nf}}{(\mu)_f}=\frac{1}{(1-\phi,)^{2.5}}, \quad (10)$$

$f,\phi_1\,and\,\phi_2$ are functions in terms of λ to be discoverd and the dash represents the derivative with respect to λ. The dimensionless forms of temperature from Eq. (5) is

$$T^*=\frac{T-T_1e^{i\omega t}}{(T_2-T_1)\,e^{i\omega t}}=Ec\left(\phi_1+\xi^2\phi_2\right).$$

The non-dimensional boundary conditions (6) in terms of f,ϕ_1,ϕ_2 g_1 and g_2 are

$$f\,(0)=1-a,f\,(1)=1,f'\,(0)=0,f'\,(1)=0,f^{''}\,(0)=0,f''\,(1)=0,$$
$$\phi_1\,(0)=0,\phi_1\,(1)=\tfrac{1}{Ec},\phi_2\,(0)=0,\phi_2\,(1)=0.$$

Table 1. Thermal physical properties of the nanoparticles and base fluid.

	Cu	Al_2O_3	Ethylene glycol
ρ	8933	3970	1110
C_P	385	765	2400
K	401	40	0.26
σ	5.96×10^7	10^{-12}	1.07×10^{-4}

§3 Numerical solution of the problem

The nonlinear ODEs (7), (8), and (9) are modified as a system of first-order differential equations as follows $(f,f',\,f'',f''',f'^v,f^v,\phi_1,\;\phi_1',\phi_2,\;\phi_2',g_1,\;g_1',g_2,\;g_2',)$=$(z_1\,z_2,\;z_3,\;z_4,\;,z_5,\;z_6,\;z_7,\;z_8,\;z_9,\;z_{10})$

$$\frac{dz_1}{d\lambda}=z_2,\frac{dz_2}{d\lambda}=z_3,\;\frac{dz_3}{d\lambda}=z_4,\frac{dz_4}{d\lambda}=z_5,\;\frac{dz_5}{d\lambda}=z_6,$$

$$\frac{dz_6}{d\lambda}=\frac{1}{\alpha^2}\frac{1}{(1-\phi)^{2.5}}z_5+A_1Re\,(z_2z_3-z_1z_4)\,cos\omega t-\frac{1}{(1-\phi)^{2.5}}Daz_3f''-A_4M^2z_3,$$

$$\frac{dz_7}{d\lambda} = z_8,$$
$$\frac{dz_8}{d\lambda} = \frac{1}{A_3}\left[\begin{array}{l} A_2 \Pr \mathrm{Re}\,(z_1 z_8)\, cos\omega t - 2A_3 z_9 - \frac{4}{(1-\phi)^{2.5}} \Pr \mathrm{Re} {z_2}^2 cos\omega t - \Pr Re\alpha^2 {z_3}^2 cos\omega t \\ -\frac{1}{(1-\phi)^{2.5}} \frac{1}{A_3} Da \Pr \mathrm{Re} {z_1}^2 cos\omega t - A_4 M^2 \Pr \mathrm{Re} {z_1}^2 cos\omega t \end{array}\right],$$
$$\frac{dz_9}{d\lambda} = z_{10},$$
$$\frac{dz_{10}}{d\lambda} = \frac{1}{A_3}\left[\begin{array}{l} A_2 \Pr \mathrm{Re}\,(-2z_2 z_9 + z_1 z_{10})\, cos\omega t - -\frac{1}{(1-\phi)^{2.5}} \Pr \mathrm{Re} {z_3}^2 cos\omega t - \Pr Re\alpha^2 {z_4}^2 cos\omega t - \\ \frac{1}{(1-\phi)^{2.5}} \frac{1}{A_3} \Pr \mathrm{Re} {z_2}^2 cos\omega t - A_4 M^2 \Pr \mathrm{Re} {z_2}^2 cos\omega t \end{array}\right]. \tag{11}$$

The initial conditions are

$$\begin{gathered} z_1(0) = 1 - a, z_2(0) = 0, z_3(0) = 0, z_4(0) = a_1, z_5(0) = a_2, \\ z_6(0) = a_3, z_7(0) = 0, z_8(0) = a_4, z_9(0) = 0, z_{10}(0) = a_5. \end{gathered} \tag{12}$$

The above differential equations system (11) is solved by using the Runge-Kutta method of fourth order under the boundary conditions (12) where a_1, a_2, a_3, a_4 and a_5 are unknown values found with the boundary condition $\lambda = 1$.

A convergence of at least 10^{-6} has been set in the calculation while using the usual Newton-Raphson method.

Shooting method.

The first step in solving the resulting BVP through (Runge-Kutta fourth order method) is to formulate system of first order equations and the corresponding initial conditions. The IVP is integrated using Runge-Kutta fourth order method by using the initial value with assumed slopes which results into a nonlinear algebraic system. Subsequently, the algebraic system is solved by using Newton-Raphson method and the values of initial slopes are found such that the boundary conditions are satisfied. It is to be noted that the choice of initial slopes plays a major role in obtaining the solution of the problem. The execution of the above thought needs an starting vector for RK4 in terms of numbers instead of symbols. Hence Newton-Raphson could be a great choice to unravel the framework of coupled nonlinear equations. The basic algorithm to compute the results is the following.

- Initialization of the parameters: Parameters and the domain of computation is defined.
- Initialization of vector for Newton-Raphson is declared and these values are substituted in the initial vector for Runge-Kutta 4th order method in the place of assumed slopes.
- The governing system of equations are declared.
- The boundary conditions are written in residual iterative loop which uses Newton-Raphson algorithm to find the accurate root such that the boundary conditions are satisfied.
- The final assumed slopes are substituted in the RK4 initial vector to obtain the required profiles.

Table 2. Nusselt number of bottom plate and top plateof Copper nanoparticles in Ethylene glycol base fluid at ωt=0.2, Da=0.3, ϕ=0.1, M=0.2.

Re	*Ec*	*Pr*	*a*	α	Nu at lower plate	Nu at Upper plate
1	0.1				8.8922	11.2634
2					3.1247	3.5618
3					1.9712	2.0214
4					1.4769	1.3613
1	0.1				8.8922	11.2634
	0.3				3.1247	3.5618
	0.5				1.9712	2.0214
	0.7				1.4769	1.3613
1	0.1	0.2	0.1	0.1	8.8922	11.2634
		0.4			7.8909	12.6484
		0.6			6.9943	14.1530
		0.8			6.1990	15.7732
1			0.1		8.8922	11.2634
			0.2		8.9818	11.2050
			0.3		9.0916	11.1280
1			0.4		9.2218	11.0326
				0.1	8.8922	11.2634
				0.2	8.8859	11.2713
				0.3	8.8735	11.2844
				0.4	8.8557	11.3025

Table 3. Comparison of current work with already published work for Newtonian fluid with suction case Terrill and Shrestha [42].

K	Re	$f''(0)$ [42]	$f''(0)$ [42]	Present $f''(0)$	$f''(1)$[42]	$f''(1)$[42]	Present $f''(1)$
0.2282	5.861	-3.22	-2.87	-3.209	0.68	0.610	0.684
0.1541	7.4277	-2.64	-2.55	-2.64	0.4176	0.4073	0.417
0.04106	13.8833	-1.233	-1.230	-1.233	0.0953	0.0951	0.0953
0.1542	31.3577	-10.12	-9.82	-10.12	0.319	0.312	0.319
0.00790	41.0960	-0.667	-0.665	-0.667	0.0166	0.0165	0.0165

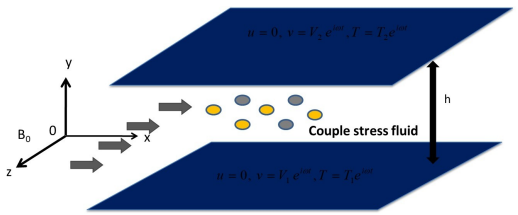

Figure 1. Geometry of the problem.

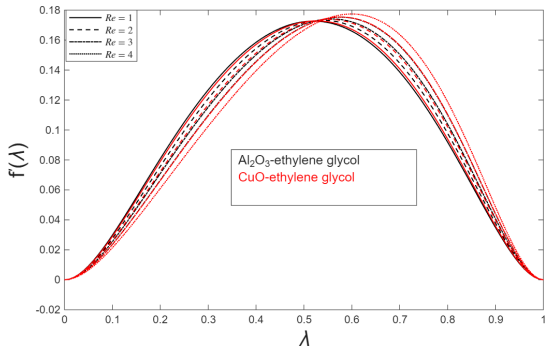

Figure 2. Effect of Re on Primary velocity.

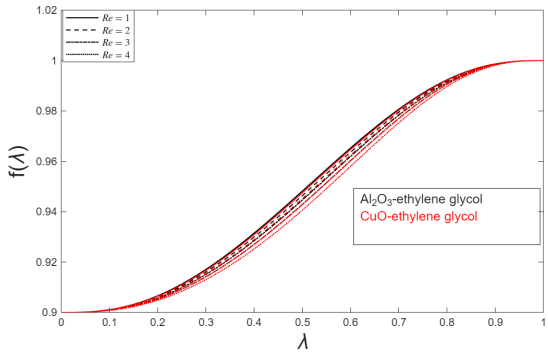

Figure 3. Effect of Re on Secondary velocity.

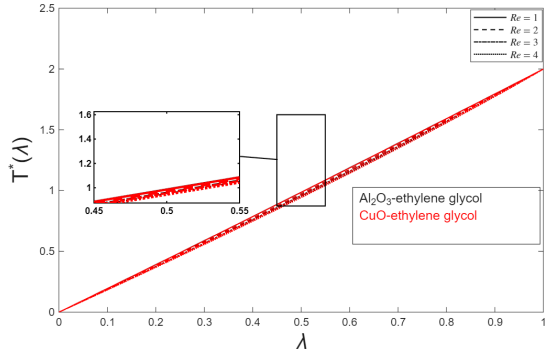

Figure 4. Effect of Re on Temperature.

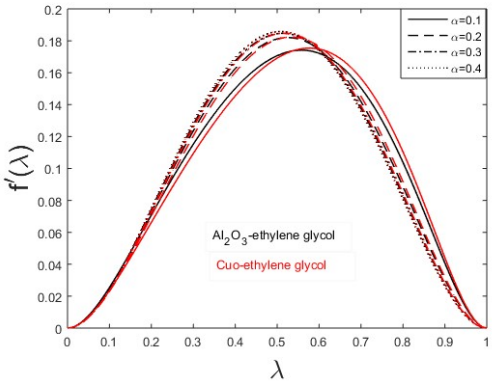

Figure 5. Effect of α on Primary velocity.

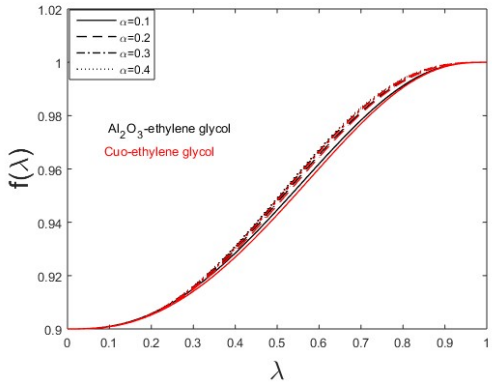

Figure 6. Effect of α on Secondary velocity.

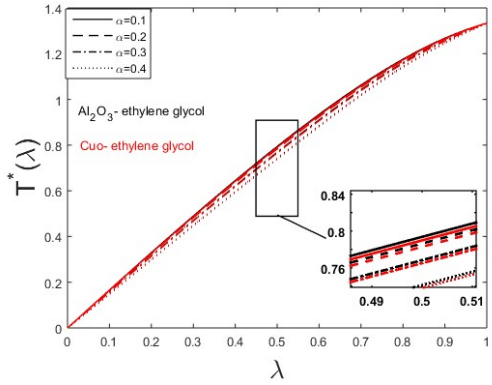

Figure 7. Effect of α on Temperature.

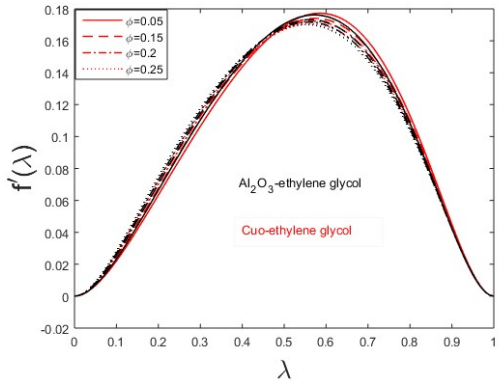

Figure 8. Effect of ϕ on Primary velocity velocity.

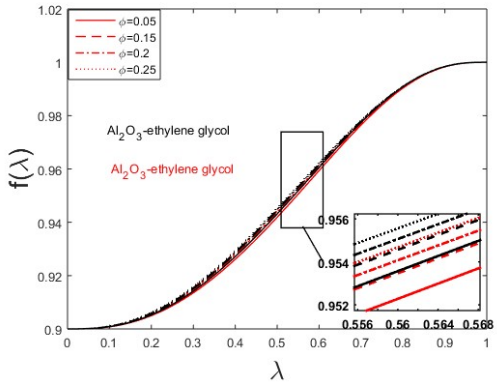

Figure 9. Effect of ϕ on Secondary velocity.

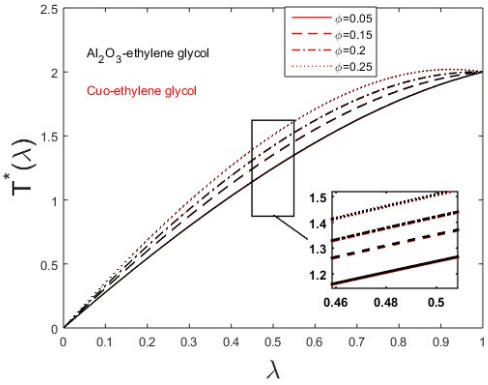

Figure 10. Effect of ϕ on Temperature.

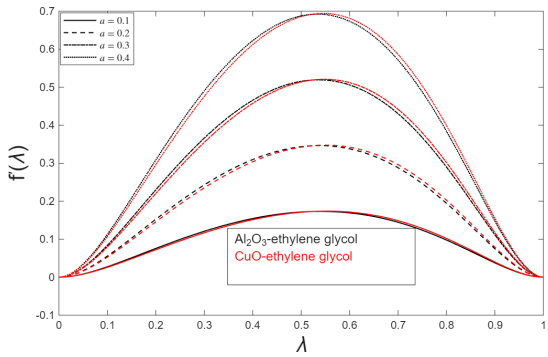

Figure 11. Effect of a on Primary velocity.

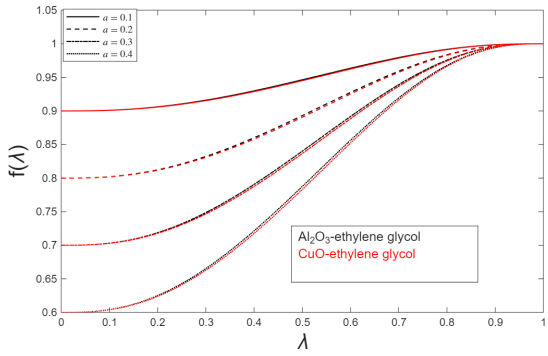

Figure 12. Effect of a on Secondary velocity.

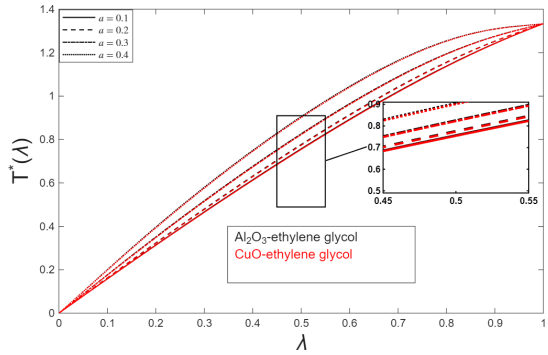

Figure 13. Effect of a on Temperature.

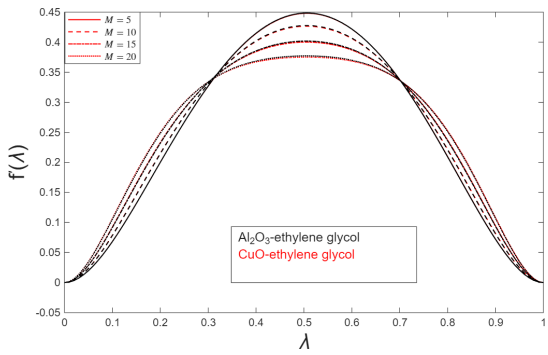

Figure 14. Effect of M on Primary velocity.

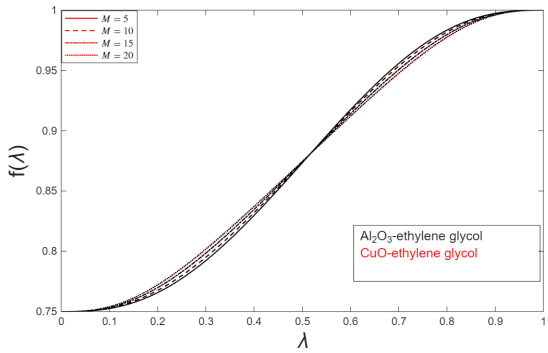

Figure 15. Effect of M on Secondary velocity.

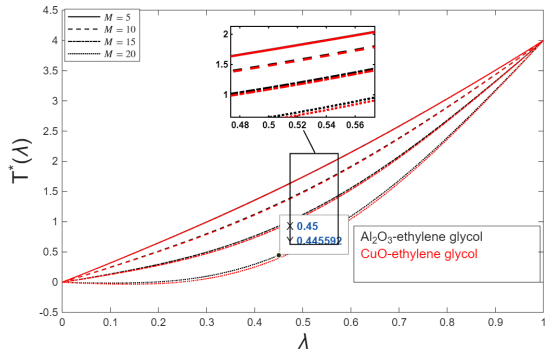

Figure 16. Effect of M on Temperature.

§4 Comprehensive discussion of the results

The ordinary differential equations (11) under the boundary conditions (12) are numerically solved by the shooting method to analyze the impact on velocity profiles, temperature profiles for Reynolds number (Re), couple stress fluid parameter (α), volume fraction(ϕ), suction-injection ratio (a) and Hartmann number (M). The obtained results are thoroughly examined and represented in the form of graphs. Heat transfer coefficient for different fluid, geometric parameters are also shown in the tables.

Figures 2, 3 and 4 show, as to how the Reynolds number behaves on primary, secondary velocity profiles and temperature distribution. The Reynolds number is a dimensionless quantity used in fluid mechanics to predict the flow patterns in different fluid flow situations. Understanding the Reynolds number is crucial in designing various engineering systems, such as pipelines, airfoil designs, and hydraulic systems, as it affects the efficiency and performance of these systems. It is observed from Fig. 2 that as Reynolds number rises the axial (primary) velocity fields decrease up to λ=0.5 and later increases. Further, the effect of Al_2O_3 nanoparticle with ethylene glycol as base fluid is more than CuO ethylene glycol nanofluids up to centre of the channel and later reverse trend is seen. It is to be noted from Fig. 3 that the secondary velocity diminishes from λ=0 to λ=1 and also radial(secondary) velocity is comparatively more for Al_2O_3 ethylene glycol nanofluids than CuO ethylene glycol nanofluid. It is due to the fact that the inertial effects are increased resulting in reduced radial velocity. This highlights the importance of inertial effects over viscous effects. The same is depicted in Fig. 3. Additionally, the temperature field shrinks as the value of Re increases as seen in Fig. 4. If we compare the temperature effects for the nano fluids considered above it is realised that aluminium oxide is generating more temperature than copper oxide nano fluid. This behaviour could be attributed to the thermal boundary layer thickness decrease which is maximum at the lower stationary plate and minimum at the upper plate.The effects of various couple stress fluid parameter (α) values on the components of velocity and temperature distribution are shown in Figs. 5, 6 and 7.

The couple stress parameter (α) in the context of couple stress fluids is a dimensionless quantity that signifies the relative importance of couple stresses compared to viscous stresses in the fluid flow. The value of α can help to identify the flow regime and predict how the fluid will behave under different flow conditions. Engineers and researchers can use (α) to design and optimize systems involving couple stress fluids, such as lubricants with additives, biological fluids (like blood), and polymeric fluids. By understanding the role of α, they can better predict the performance and efficiency of these systems. It has been noted from Fig. 5 that, when the couple stress fluid parameter grows, the axial velocity component climbs up till the channel's centre, located at λ=0.5 before declining as the parameter rises and also Al_2O_3 nanoparticle produces more primary velocity than CuO upto the centre of the channel and later a reverse trend is observed. For the radial velocity profile an enhancement from lower plate (λ=0) to upper plate (λ=1) is observed which acn be seen in Fig. 6. Also Al_2O_3 nanoparticles result in more radial velocity. However, the temperature distribution decreases from lower plate (λ=0) to top plate (λ=1) with growing of α. This is due to the fact the enhancement in couple stress

parameter results in greater stress among all the coupled fluid particles, which has a tendency to reduce the temperature profile as depicted in Fig. 7. The effect of ϕ (volume fraction) on the velocity components and temperature distribution is shown in Figs. 8, 9 and 10. The volume fraction refers to the proportion of nanoparticles dispersed in the base fluid. It is a crucial parameter because it significantly influences the thermal, rheological, and physical properties of the nanofluid. The volume fraction ϕ is defined as the ratio of the volume of nanoparticles to the total volume of the nanofluid. It is usually expressed as a percentage or a decimal. The conclusion from Fig. 8 is that the axial velocity profile rises as λ approaches the channel's centre where λ=0.5 and then it falls with increase of volume fraction. As identified earlier Al_2O_3 nanoparticle is more effective than CuO nanofluids up to centre of the channel with reverse trend subsequently. Whereas the radial velocity profile and temperature distribution are boosted from bottom plate (λ=0) to top plate (λ=1) with the raise in the value of ϕ (volume fraction) and if we see comparison of two nanofluids for radial velocity profile and temperature distribution, Al_2O_3 ethylene glycol nanofluids is having more impact than Cuo ethylene glycol nanofluid. The same have been pictured in Figs. 9 and 10 respectively. Increasing the volume fraction of nanoparticles generally enhances the thermal conductivity of the nanofluid due to the higher thermal conductivity of the solid particles compared to the base fluid.

The significance of different values of a (suction and injection ratio) on velocity components and the temperature distribution can be seen in Figs. 11, 12 and 13. the suction and injection ratio is a dimensionless parameter that characterizes the effect of fluid being either injected into or sucked out of the boundary layer through a porous surface. This parameter is crucial for understanding how these actions influence the flow characteristics, such as boundary layer thickness, stability, and heat transfer. Aerospace Engineering: Suction and injection are used in aircraft design to control boundary layer separation and reduce drag, improving fuel efficiency and performance.

Cooling systems: Injection of cool fluid or suction of heated fluid can be used to manage thermal loads in high-performance electronic systems and industrial processes. Environmental engineering: Control of suction and injection is applied in pollutant dispersion and soil remediation technique.

It is depicted that the axial velocity profile increases as one approaches the channel's centre λ=0.5 and then starts diminishing from there onwards till the end of the channel. Also Al_2O_3 nanoparticle is enhancing the axial velocity profile more than that of CuO nanofluid up to centre of the channel with a reverse trend subsequently till the end of the channel as can be seen from Fig. 11. However as the value of 'a' rises, the radial velocity profile declines. across the channel. Also, Al_2O_3 based nanofluids produce more impact on radial velocity in tyhe form increasing it when compared to CuO based nanofluid. Both these effects are shown graphically in Fig. 12. Also, as the value of the suction to injection ratio rises, the temperature distribution also does behave in the similar manner. This is pictured in Fig. 13. Physically it can be justified that the the radial velocity component between the plates decreased as a result of the decrease in suction velocity whenever 'a' increases. The Hartmann number M impact on the velocity and temperature profiles is seen in Figs. 14, 15 and 16. The Hartmann number M is a dimensionless quantity used in magnetohydrodynamics to characterize the influence of a magnetic field on a

conducting fluid flow. The Hartmann number is used to design and control MHD systems, such as MHD pumps and generators, by tuning the magnetic field to achieve desired flow characteristics. As M increases the axial velocity also increases with Al_2O_3 nanoparticle is showing more impact than CuO ethylene glycol nanofluids up to centre of the channel with a reverse trend later. Increasing the Hartmann number, the radial velocity field decreases with Al_2O_3 ethylene glycol nanofluids out performing CuO ethylene glycol nanofluids. It is evident that when the value of M increases, there is a tendency for the fluid flow to slow down, which is consistent with physical reality, because there is a transverse magnetic field present, which in turn produces a resistive force akin to the drag force that acts in the opposite direction to the flow of fluids. This suggests that the flow field is delayed by the imposed magnetic field. However, the temperature field increases with an increase in M. Table I represents the thermal physical properties of the nanopraticales and the base fluid. Table II indicates, the computed Nusselt number at bottom and top plates for Copper nanoparticles. It is understood from the table that the heat transfer rate at the lower plate increases for only the suction/injuction Ratio (a) but falls for Re, Ec, Pr, and α. The heat transfer rate for the upper plate is growing for Pr and α, whereas it is decreasing for Re, Ec, and a. Table III represents the comparison our results with previously published work of Terrill and Shrestha [42]. We reduce our problem to viscous fluid model by considering Couple Stress Fluid parameter (α) , fluid friction (ϕ), Darcy parameter (Da), Hartmann number (M) as zero. It is found that there is a good agreement between the results obtained in the reduced model and that of Terrill and Shrestha[42], thus validating the results of the present work and also justifies the methodology in the present analysis.

§5 Conclusions

The results are examined for the geometric parameters as well as the non-dimensional velocity profile, energy characteristics and Nusselt number with regard to various fluid parameters. The significant findings can be summed up as follows.

- As the Hartmann number increases, the temperature profiles rise as well.
- With the increase in the suction injection ratio, we observe that the temperature profiles also show an increasing trend, although with Reynolds numbers it show the opposite trend.
- As the value of the volume fraction rises, the temperature profiles also show similar pattern.
- As the Reynolds number increases the coefficient of skin friction at the upper and lower plate decreases.
- The presence of couple stresses in the fluid increases the Radial velocity and decreases the temperature.

- Al_2O_3 based nanofluids produce more impact on Temperature when compared to CuO based nanofluids at any Hartmann number.
- When the fluid friction as well as Suction/Injection parameters are increased, the temperature distribution of the fluid increases; however, this trend reverses at Hartmann number parameter values.
- The increase in Nusselt number at upper plate was found to be the resultant of the rise seen in the Prandtl number.
- The method adopted as well as the results obtained have been validated and are found to be agreeing well with the existing literature.

Declarations

Conflict of interest The authors declare no conflict of interest.

References

[1] V K Stokes. *Couple stresses in fluids*, Physics of Fluids, 1966, 9(9): 1709-1715.

[2] V K Stokes. *Micropolar Fluids. In Theories of Fluids with Microstructure*, Heidelberg: Springer Berlin, 1984, 150-178.

[3] M Devakar, T K V Iyengar. *Run up flow of a couple stress fluid between parallel plates*, Nonlinear Analysis: Modelling and Control, 2010, 15(1): 29-37.

[4] M S Sarojini, M V Krishna, C U Shankar. *MHD flow of a couple stress fluid through a porous medium in a parallel plate channel in presence of effect of inclined magnetic field*, International Journal of Physics and Mathematical Sciences, 2011, 1(1): 9-18.

[5] D Srinivasacharya, N Srinivasacharyulu, O Odelu. *Flow of couple stress fluid between two parallel porous plates*, International Journal of Applied Mathematics, 2011, 41: 10-14.

[6] J R Murthy, J Srinivas. *First and second law analysis for the MHD flow of two immiscible couple stress fluids between two parallel plates,* Heat Transfer Asian Research, 2015, 44(5): 468-487.

[7] M Devakar, D Sreenivasu, B Shankar. *Analytical solutions of couple stress fluid flows with slip boundary conditions,* Alexandria Engineering Journal, 2014, 53(3): 723-730.

[8] K Ramesh. *Influence of heat and mass transfer on peristaltic flow of a couple stress fluid through porous medium in the presence of inclined magnetic field in an inclined asymmetric channel,* Journal of Molecular Liquids, 2016, 219: 256-271.

[9] S U S Choi, J A Eastman. *Enhancing thermal conductivity of fluids with nanoparticles,* ASME International Mechanical Engineering Congress & Exposition, 1995, 219: 12-17.

[10] M Sheikholeslami, D D Ganji. *Heat transfer of Cu-water nanofluid flow between parallel plates*, Powder Technology, 2013, 235: 873-879.

[11] T Hayat, T Muhammad, A Alsaedi, et al. *Magnetohydrodynamic three-dimensional flow of viscoelastic nanofluid in the presence of nonlinear thermal radiation*, Journal of Magnetism and Magnetic Materials, 2015, 385: 222-229.

[12] A S Dogonchi, K Divsalar, D D Ganji. *Flow and heat transfer of MHD nanofluid between parallel plates in the presence of thermal radiation*, Computer Methods in Applied Mechanics and Engineering, 2016, 310: 58-76.

[13] T Hayat, R Sajjad, T Muhammad, et al. *On squeezed flow of couple stress nanofluid between two parallel plates*, Results in Physics, 2017, 7: 553-561.

[14] M Kumar, K P Kashya, N N Kumar. *Effect of magnetite nanoparticles on couple stress fluid between two parallel squeezing and expanding surfaces*, SN Applied Sciences, 2020, 2: 848.

[15] R Arpitha, D Srikanth. *Temperature and Mass Dispersion of Free Convective Radiative Non-Newtonian Nano Fluid Flow between Two Parallel Plates*, Indian Journal of Pure & Applied Physics, 2022, 60(6): 497-508.

[16] A Khan, M A Alyami, W Alghamdi, et al. *Thermal examination for the micropolar gold-blood nanofluid flow through a permeable channel subject to gyrotactic microorganisms*, Frontiers in Energy Research, 2022, 10: 993247.

[17] A Khan, Z Iqbal, T Gul, et al. *Influences of radiative heat transfer on hydromagnetic hybrid nanofluid flow through two rotating surfaces*, Thermal Science, 2023, 27(1): 227-236.

[18] A Khan, Z Iqbal, N A Ahammad, et al. *Bioconvection Maxwell nanofluid flow over a stretching cylinder influenced by chemically reactive activation energy surrounded by a permeable medium*, Frontiers in Physics, 2023, 10: 1065264.

[19] I Ali, T Gul, A Khan. *Unsteady hydromagnetic flow over an inclined rotating disk through neural networking approach*, Mathematics, 2023, 11(8): 1893.

[20] N W Khan, A Khan, M Usman, et al. *Influences of Marangoni convection and variable magnetic field on hybrid nanofluid thin-film flow past a stretching surface*, Chinese Physics B, 2022, 31(6): 064403.

[21] A Khan, Z Shah, S Islam, et al. *Darcy-Forchheimer flow of micropolar nanofluid between two plates in the rotating frame with non-uniform heat generation/absorption*, Advances in Mechanical Engineering, 2018, 10(10): 1-16.

[22] A Khan, Z Shah, E Alzahrani, et al. *Entropy generation and thermal analysis for rotary motion of hydromagnetic Casson nanofluid past a rotating cylinder with Joule heating effect*, International Communications in Heat and Mass Transfer, 2020, 119: 104979.

[23] S Islam, A Khan, W Deebani, et al. *Influences of Hall current and radiation on MHD micropolar non-Newtonian hybrid nanofluid flow between two surfaces*, AIP Advances, 2020, 10(5): 055015.

[24] S Farooq, M I Khan, A Riahi, et al. *Modeling and interpretation of peristaltic transport in single wall carbon nanotube flow with entropy optimization and Newtonian heating*, Computer Methods and Programs in Biomedicine, 2020, 192: 105435.

[25] M Nazeer, M I Khan, M U Rafiq, et al. *Numerical and scale analysis of Eyring-Powell nanofluid towards a magnetized stretched Riga surface with entropy generation and internal resistance*, International Communications in Heat and Mass Transfer, 2020, 119: 104968.

[26] Y M Chu, S Jakeer, S R R Reddy, et al. *Double diffusion effect on the bio-convective magnetized flow of tangent hyperbolic liquid by a stretched nano-material with Arrhenius Catalysts*, Case Studies in Thermal Engineering, 2023, 44: 102838.

[27] M Nazeer, F Hussain, Q Shahzad, et al. *Perturbation solution of the multiphase flows of third grade dispersions suspended with Hafnium and crystal particles*, Surfaces and Interfaces, 2021, 22: 100803.

[28] Y M Chu, F Shah, M I Khan, et al. *Cattaneo-Christov double diffusions (CCDD) in entropy optimized magnetized second grade nanofluid with variable thermal conductivity and mass diffusivity*, Journal of Materials Research and Technology, 2020, 9(6): 13977-13987.

[29] M I Khan, H Waqas, U Farooq, et al. *Assessment of bioconvection in magnetized Sutterby nanofluid configured by a rotating disk: a numerical approach*, Modern Physics Letters B, 2021, 35(12): 2150202.

[30] H Vaidya, K V Prasad, M I Khan, et al. *Combined effects of chemical reaction and variable thermal conductivity on MHD peristaltic flow of Phan-Thien-Tanner liquid through inclined channel*, Case Studies in Thermal Engineering, 2022, 36: 102214.

[31] H A Attia, N A Kotb. *MHD flow between two with heat transfer parallel plates*, Acta Mechanica, 1996, 117(1): 215-220.

[32] T Hayat, M U Qureshi, Q Hussain. *Effect of heat transfer on the peristaltic flow of an electrically conducting fluid in a porous space*, Applied Mathematical Modelling, 2009, 33(4): 1862-1873.

[33] D K Kaladhar. *Mixed convection flow of couple stress fluid between parallel vertical plates with Hall and Ion-slip effects*, Communications in Nonlinear Science and Numerical Simulation, 2012, 17(6): 2447-2462.

[34] S O Adesanya, O D Makinde. *Heat transfer to magnetohydrodynamic non-Newtonian couple stress pulsatile flow between two parallel porous plates*, Zeitschrift für Naturforschung, 2012, 67a: 647-656.

[35] S T Mohyud-Din, U Khan, N Ahmed, et al. *A study of heat and mass transfer on magnetohydrodynamic (MHD) flow of nanoparticles*, Propulsion and Power Research, 2018, 7(1): 72-77.

[36] N A Khan, S Aziz, N A Khan. *Numerical simulation for the unsteady MHD flow and heat transfer of couple stress fluid over a rotating disk*, Plos One, 2014, 9(5): e95423.

[37] J Raza, A M Rohni, Z Omar. *MHD flow and heat transfer of Cu-Cwater nanofluid in a semi porous channel with stretching walls*, International Journal of Heat and Mass Transfer, 2016, 103: 336-340.

[38] O Ojjela, K Ramesh, S K Das. *Second law analysis of MHD squeezingflow of Casson fluid between two parallel disks*, International Journal of Chemical Reactor Engineering, 2018, 16(6): 20170163.

[39] A Raptis, C Massalas, G Tzivanidis. *Hydromagnetic free convection flow through a porous medium between two parallel plates*, Physics Letters A, 1982, 90(6): 288-289.

[40] A Gbadeyan, M Dada. *On the influence of radiation and heat transfer on an unsteady MHD non-Newtonian fluid flow with slip in a porous medium*, Journal of Mathematics Research, 2013, 5(3): 40-50.

[41] K Ramesh, M Devakar. *Magnetohydrodynamic peristaltic transport of couple stress fluid through porous medium in an inclined asymmetric channel with heat transfer*, Journal of Magnetism and Magnetic Materials, 2015, 394: 335-348.

[42] R M Terrill, G M Shrestha. *Laminar flow through a channel with uniformly porous walls of different permeability*, Applied Scientific Research, 1966, 15: 440-468.

Department of Applied Mathematics, Defence Institute of Advanced Technology (Deemed to be University), Pune-411025, India.

Email: dasarisrikanth@diat.ac.in